British Journal of Pharmacology

British Journal of Pharmacology (2018) **175** 631–643 631

RESEARCH PAPER

Achyranthes bidentata polypeptide protects dopaminergic neurons from apoptosis in Parkinson's disease models both *in vitro* and *in vivo*

Correspondence Professor Cheng Sun, Key Laboratory of Neuroregeneration of Jiangsu Province and Ministry of Education, Co-Innovation Center of Neuroregeneration, Nantong University, 19 Qixiu Road, Nantong, Jiangsu 226001, China. E-mail: suncheng1975@ntu.edu.cn

Received 17 March 2017; **Revised** 14 November 2017; **Accepted** 19 November 2017

Su Peng*, Caiping Wang*, Jinyu Ma*, Ketao Jiang, Yuhui Jiang, Xiaosong Gu and Cheng Sun

Key Laboratory of Neuroregeneration of Jiangsu Province and Ministry of Education, Co-Innovation Center of Neuroregeneration, Nantong University, Nantong, Jiangsu China

*These authors contributed equally to this work.

BACKGROUND AND PURPOSE

Parkinson's disease (PD) is a neurodegenerative disorder closely associated with dopaminergic neuron loss. It is well documented that *Achyranthes bidentata* polypeptides (ABPP) are potent neuroprotective agents in several kinds of neurons. Therefore, we proposed that ABPP might play a beneficial role against PD by protecting dopaminergic neurons from apoptosis.

EXPERIMENTAL APPROACH

SH-SY5Y cells and primary rat dopaminergic neurons were pretreated with ABPP fraction k (ABPPk), a purified fraction of ABPP, and then the cells were exposed to 1-methyl-4-phenylpyridinium iodide (MPP^+) to induce apoptosis. Cell viability, LDH activity, a Tunel assay and protein levels of Bcl-2 and Bax were analysed. In an *in vivo* PD model induced by MPTP, ABPPk was intranasally delivered to mice. Behavioural tests, immunohistochemistry, immunostaining, Nissl staining, qRT-PCR and Western blot were employed to evaluate the potential effects of ABPPk on PD in mice.

KEY RESULTS

The application of ABPPk markedly enhanced the viability of SH-SY5Y cells and primary dopaminergic neurons treated with neurotoxic agent MPP^+. In an *in vivo* MPTP-induced PD model, ABPPk significantly improved behavioural performances and prevented tyrosine hydroxylase loss in the substantia nigra pars compacta and striatum. Furthermore, we showed that MPTP-induced astrocyte and microglia activation were largely attenuated by ABPPk, leading to low levels of neuroinflammation and a downregulation of the apoptotic signalling pathway.

CONCLUSION AND IMPLICATIONS

Taken together, our data show that ABPPk protects dopaminergic neurons from apoptosis, suggesting that ABPPk might be an effective intervention for treating the neuron loss associated with disorders such as PD.

Abbreviations

ABPPk, *Achyranthes bidentata* polypeptide fraction k; MPP^+, 1-methyl-4-phenylpyridinium iodide; MPTP, 1-methyl-4-pheynl-1,2,3,6-tetrahydropyridine hydrochloride; MTT, 3-(4,5-dimethylthiazol-2-yl)-2,5-diphenyltetrazolium bromide; PD, Parkinson's disease; SNpc, substantia nigra pars compacta

DOI:10.1111/bph.14110

Introduction

Parkinson's disease (PD) is a common neurodegenerative disorder characterized by progressive loss of midbrain dopaminergic neurons. In the early stages of this disease, the most obvious symptoms are movement-related, such as shaking, slowness of movement and difficulty with walking and gait. Later, thinking and behavioural problems may arise, with dementia and depression occurring in the advanced stages of the disease. PD is more common in older people with most cases occurring after the age of 50. In 2013, PD resulted in about 103 000 deaths globally, up from 44 000 deaths in 1990 (Mortality GBD and Causes of Death C, 2015). The molecular mechanisms underlying the pathology of PD are still poorly understood (Goedert, 2015; Makin, 2016). At present, PD cannot be completely cured, and prescription drugs such as dopamine agonists and **monoamine oxidase** (MAO-B) inhibitors only have limited efficacy at the early stages of PD. Thus, it is of great importance to develop novel therapeutic agents for PD.

Achyranthes bidentata has long been used to treat various human diseases, particularly in China, Japan and Korea. Several bioactive substances have been isolated from *A. bidentata* (Shen *et al.,* 2010; Zou *et al.,* 2011; He *et al.,* 2014). *A. bidentata* polypeptide (ABPP) is one such substance that has been extensively studied by our group. For example, Shen *et al.* reported the protective effects of ABPP against **NMDA**-induced cell apoptosis in cultured hippocampal neurons (Shen *et al.,* 2008, 2010); in addition, we previously showed that ABPP protects neurons from serum and/or glucose deprivation *in vitro* and *in vivo* (Shen *et al.,* 2011, 2013; Yu *et al.,* 2014). Besides the CNS, ABPP also plays an important role in the peripheral nervous system to promote sciatic nerve regeneration after injury (Yuan *et al.,* 2010; Wang *et al.,* 2013; Cheng *et al.,* 2014). Recently, by further purifying ABPP using HPLC, a fraction that exhibits excellent neuron-protective efficiency was identified and subsequently named as ABPP fraction k (ABPPk; Yu *et al.,* 2014). Since ABPP is known to contain excellent neuron-protective efficiency, it is reasonable to predict that ABPPk may have beneficial effects for treating neurodegenerative disorders such as PD.

In this study, we used both *in vitro* and *in vivo* PD models to investigate the potential anti-Parkinson activity of ABPPk. Our results showed that ABPPk treatment markedly protects dopaminergic neurons from apoptosis induced by neurotoxic agent **MPP^+**. Moreover, the application of ABPPk *in vivo* improved behavioural performances and attenuated microglia and astrocyte activation in a mouse model of PD. These beneficial effects of ABPPk against PD probably depend on its modulating effects on neuroinflammation. We suggest that ABPPk has the potential to be a useful intervention for preventing the loss of dopaminergic neurons associated with disorders such as PD.

Methods

Blinding, group size and randomization

The data analyst was blinded, whereas the experimental performers were generally not blind to group information. Mice were randomly divided into the experimental groups (n = 5 for each group). Quantitative analysis of gene and protein expression was normalized to the mean of the control group. Quantitative-PCR data were adjusted by using a reference gene 18S. The bands of interest in the Western blots were normalized to tubulin or actin or total protein. Relative mRNA and protein levels are expressed as fold of control mean.

Compliance with requirements for animal experiments

Animal protocols followed the Guide for the Care and Use of Laboratory Animals (US Department of Health, NIH) and were approved by the Animal Care and Use Committee of Nantong University and the Jiangsu Province Animal Care Ethics Committee. Animal studies are reported in compliance with the ARRIVE guidelines (Kilkenny *et al.*, 2010; McGrath and Lilley, 2015).

Animals were housed in the animal-specific pathogen-free facility in cages with standard wood-based bedding and space (five mice per cage). Eight-week-old male C57BL/6J mice were selected for the experiments in this study. The housing environment was maintained at 22–24°C and 55–60% relative humidity. The mice had free access to food and drinking water and 12 h shift between light and darkness. At the end of treatment, all mice were killed by an overdose of isoflurane anaesthetic, followed by cervical dislocation. No mice were excluded from statistical analysis.

ABPPk isolation and purification

The roots of *A. bidentata* blume were purchased from a local Chinese medicine grocery and identified by Prof. Haoru Zhao from China Pharmaceutical University. The extraction procedures for crude ABPP were as described previously (Shen *et al.,* 2008). The fraction ABPPk was purified by HPLC (Cheng *et al.,* 2014; Yu *et al.,* 2014).

Cell culture and treatment

SH-SY5Y cells were obtained from ATCC and cultured in DMEM supplemented with 10% FBS and incubated at 37°C in a humidified atmosphere with 5% CO_2. Primary rat midbrain dopaminergic neurons were prepared as described elsewhere (Gandhi *et al.,* 2009). In brief, animals were killed by cervical dislocation under anaesthesia, their brains were quickly removed, and the midbrain was harvested on a cold stage. The mesencephalic tissues procured were digested by 0.25% trypsin in Ca^{2+}- and Mg^{2+}-free HBSS at 37°C for 10 min, and the resulting cell suspension was passed through a filter and centrifuged at 200 × g for 5 min. The cells were re-suspended in DMEM supplemented with 10% FBS and plated onto a poly-L-lysine-coated plate in a humidified atmosphere of 95% air and 5% CO_2 at 37°C for 4 h. Then, the culture medium was replaced by Neurobasal medium supplemented with 2% B27. The maturation of mesencephalic neurons required 7–8 days with medium changes every 2 days. Cells were pretreated with ABPPk at different dosages (25, 50 and 100 ng·mL^{-1}). After a 12 h pretreatment with ABPPk, SH-SY5Y cells and primary dopaminergic neurons were exposed to 500 and 50 μM of MPP^+ for 36 h, respectively, to induce cell apoptosis. The MPP^+ dosages employed were similar to those

used previously with a slight modification (Aime *et al.*, 2015; Ye *et al.*, 2016).

Cell viability assay

Cell viability was measured by the 3-(4,5-dimethylthiazol-2-yl)-2,5-diphenyltetrazolium bromide (MTT) assay. Cells were seeded in 96-well plates at 1×10^4 cells per well. After overnight incubation, plates were incubated with MPP^+ for 36 h after a 12 h pretreatment with ABPPk. The concentrations of toxic agents and ABPPk are indicated in the figure legends. Subsequently, the medium was removed, a final concentration of 500 $\mu g \cdot mL^{-1}$ MTT was added to each well, and cells were incubated at 37°C for 4 h, and then cells were lysed in 10% SDS with incubation at 37°C for 20 h. Absorbance at 570 nm was measured in a microplate reader (BioTek, USA).

Tunel staining of apoptotic cells

Tunel analysis was performed using the *In Situ* Cell Death Detection kit (Roche, Penzberg, Germany) according to the manufacturer's instructions. Cells were fixed in 4% paraformaldehyde for 1 h and then incubated in permeabilization solution for 2 min on ice. After three washes, 100 μL DNase 1 (1500 $U \cdot mL^{-1}$) were added to the positive control group and incubated in a wet box for 20 min. A total of 500 μL Tunel reaction mixture solution (50 μL enzyme solution +450 μL label solution) was added to the positive control group and the experimental group, and 50 μL label solution were added to the negative control group. The sections were incubated in the dark in the wet box for 60 min. Differential interference contrast microscopy images were then obtained at 20× magnification following the random selection. The number of apoptotic cells and total cells were counted, and then the cell apoptosis rate was determined by the following equation: cell apoptosis rate (%) = the number of apoptotic cells/total cells × 100.

LDH assay

LDH activity in cell culture medium was determined by a commercial kit according to the manufacturer's instructions, as described previously (Xie *et al.*, 2015). Briefly, the cell culture medium was collected and treated with LDH-assay reaction mixture for 30 min at room temperature in the dark. The absorbance was measured with a microplate reader (BioTek, USA) at 490 nm. The cell death ratio was calculated by the following formula according to the manufacturer's instructions: cell death ratio (%) = $(A_{sample} - A_{blank})/(A_{max} - A_{blank}) \times 100$.

A_{sample} = sample absorbance value;

A_{blank} = the absorbance value of blank group;

A_{max} = the absorbance value of positive group.

The cell death ratio was expressed as LDH release.

Animals

Eight-week-old male C57BL/6J mice were used to evaluate the potential protective effects of ABPPk on MPTP-induced dopaminergic neurotoxicity. Twenty mice were used for each experiment, of which 10 mice were randomly selected for treating with saline and 10 mice were treated with MPTP (20 $mg \cdot kg^{-1}$) *via* i.p. injection at a 24 h interval, for seven consecutive days. For long-term experiments, mice were injected with MPTP at the dosage of 30 $mg \cdot kg^{-1}$. The saline group and MPTP group were randomly divided into two groups (n = 5 for each group). ABPPk was delivered intranasally (i.n.) three times a week for 2 weeks. Mice were briefly anaesthetized with 1.5% isoflurane, and ABPPk at the dosage of 100 $\mu g \cdot kg^{-1} \cdot day^{-1}$ (total volume of 20 μL) was administered i.n. to C57BL/6J mice, 3 μL at a time, alternating the nostrils, with a lapse of 2 min between each administration. In the control mice, saline (0.9% $w \cdot v^{-1}$) was administered. Then a total of four subgroups were generated: (i) Saline i.p. + saline i.n. (SHAM + vehicle); (ii) Saline i.p. + ABPPk i.n. (SHAM + ABPPk); (iii) MPTP i.p. + saline i.n. (MPTP + vehicle); and (iv) MPTP i.p. + ABPPk i.n (MPTP + ABPPk).

Behavioural tests

The rotarod test was performed using an accelerating rotarod apparatus (model LE8500; Panlab) as described previously (Choi *et al.*, 2013). The mice were trained for two consecutive days before MPTP injections in an acceleration mode (4–40 rpm) over 5 min. The training was repeated with a constant speed (16 rpm) until the mice were able to stay on the rod for at least 300 s. For the formal test, mice were placed on a rotating drum, accelerated from 4 to 40 rpm over a 5 min period. Time spent moving on the rod was recorded before falling was measured. The pole test was conducted with the method described elsewhere (Choi *et al.*, 2013). Briefly, mice were held on the top of a pole (diameter 16 mm; height 60 cm) with a rough surface. Mice were habituated to the task 1 day before testing. On the test day, the total time taken to descend was measured and considered as locomotor activity. The test was conducted in triplicate, and the average values were used for each animal.

Tissue collection and preparation

Mice were perfused transcardially with ice-cold PBS (0.1 M, pH 7.4) after deep anaesthesia with isoflurane. The brains were immediately extracted and cut sagittally into hemispheres. One hemisphere was fixed overnight in 4% PFA and then dehydrated in 10% and 30% sucrose in PBS at 4°C for immunofluorescence and immunohistochemistry analysis. The other hemisphere was further dissected into substantia nigra pars compacta (SNpc) and striatum under a stereomicroscope, according to the mouse brain atlas (Franklin and Paxinos, 2008). The SNpc and striatum were then immediately frozen in liquid nitrogen and kept at −80°C until used.

Immunohistochemistry, Nissl staining and stereological estimation

Mice were deeply anaesthetized with isoflurane, and then the brains were immediately removed. Next, tissues were fixed in phosphate-buffered 4% paraformaldehyde, pH 7.4, at 4°C. Fixed brains were cut on a vibratome set at 12 μm, and tissue sections were incubated overnight with mouse anti-tyrosine hydroxylase (**TH**) at 4°C. They were then incubated with

biotinylated anti-mouse IgG for 1 h followed by 1 h-incubation in ABC solution at 37°C. The peroxidase activity was visualized with 3,3′-Diaminobenzidine in 50 mM tris-buffered saline (pH 7.6). For Nissl staining, paraffin sections were deparaffinized and hydrated, stained with methylene blue buffer for 10 min and then immersed in acetic acid buffer for 2 min. Pictures were taken using a light microscope (Leica, DM2500 LED) at a magnification of 5×. The total number of TH-positive and Nissl-stained cells were counted by unbiased stereology method as described elsewhere (Nam *et al.,* 2015; Alam *et al.,* 2017). Briefly, TH- and Nissl-positive cells were counted using the optical fractionator performed on a bright field microscope (Leica, DM2500 LED) using Stereo Investigator software (MBF Bioscience). A counting frame of 50 × 50 μm with framing space of 200 μm and a height of 10 μm was chosen. Only the cells that came into focus within the counting frame height were counted. At least 50 markers were counted within 50 framing sites for each animal.

Immunostaining

Midbrain sections (12 μm in thickness) were prepared from brain tissue fixed with 4% paraformaldehyde and immunostaining was as performed as previously described (Liu *et al.,* 2017). Antibodies used for the immunostaining were glial fibrillary acidic protein (GFAP) and CD68. In each section, four to six images were taken using confocal microscopy (Zeiss microscope; Carl Zeiss Microimaging, GmbH). The fluorescence intensity was quantified using Image J software. The backgrounds were subtracted using the Process/Substract Background function for each image. The average fluorescence intensity was calculated from 10 regularly distributed areas in the sample images.

RNA extraction and quantitative real time PCR (qRT-PCR)

Total RNA was extracted from cells or animal tissues using Trizol reagent (Invitrogen) and transcribed into cDNA using cDNA synthesis kit (Bio-Rad). The gene expression analysis was performed with iQ5 Multicolor Real-Time PCR Detection System (Bio-Rad) with SYBR Green Supermix (Bio-Rad). The mRNA level was calculated by the $2^{-\Delta\Delta CT}$ method and normalized to the expression of 18S. The primer sequences used were as follows:

Gene	Forward primer	Reverse primer
18S	AGTCCCTGCCCTT TGTACACA	CGTTCCGAGGGCC TCACT
IL-1a	GTGTTGCTGAA GGAGTTG	ATCTGGAAGTCT GTCATAGAG
IL-1b	GCAACTGTTCC TGAACTCAACT	ATCTTTTGGGGTC CGTCAACT
IL-12a	CAATCACGCTACC TCCTCTTTT	CAGCAGTGCAGG AATAATGTTTC
IL-10	GAAGAGAAACCA GGGAGAT	GCAGACAAACAATA CACCAT

Cell and tissue protein extraction

Cell and tissue protein extraction was as described elsewhere (Liu *et al.,* 2016). Briefly, tissues were homogenized with a bench-top homogenizer (Polytron, PT2100) in ice-cold tissue lysis buffer (25 mM Tris–HCl, pH 7.4; 100 mM NaF; 50 mM $Na_4P_2O_7$; 10 mM Na_3VO_4; 10 mM EGTA; 10 mM EDTA; 1% NP-40; 10 $\mu g \cdot mL^{-1}$ leupeptin; 10 $\mu g \cdot mL^{-1}$ aprotinin; 2 mM PMSF and 20 nM okadaic acid). After homogenization, lysates were rotated for 1 h at 4°C and then subjected to centrifugation at 13 800 × *g* for 20 min at 4°C. The lipid layer was removed, and the supernatant was transferred into Eppendorf tubes for centrifugation. Protein concentration was quantified by using a Protein Assay Kit (Bio-Rad). Equivalent protein concentration in each sample was prepared and boiled at 100°C for 5 min in 1× Laemmli buffer. The lysates were cooled to room temperature before loading for Western blot analysis.

Western blot analysis

Western blot analysis was performed as previously described (Sun *et al.,* 2014). Samples from cell lysates or tissue lysates were resolved by SDS-PAGE and then transferred to a PVDF membrane. After 1 h blocking at room temperature using 10% blocking reagent (Roche), the membrane was incubated overnight with primary antibody (1:1000 dilution) in Tris-buffered saline solution/Tween (TBST) containing 10% blocking reagent at 4°C. After the incubation, the membrane was washed three times in TBST and incubated with secondary antibody (1:10 000 dilution) for 1 h at room temperature. After three washes in TBST, the membrane was developed using a chemiluminescence assay system (Roche) and exposed to Kodak film. Blots were quantified by the Image J programme and the bands of interest were normalized to those of tubulin, actin or total protein, as indicated in each figure. For stripping the membrane, it was vigorously shaken in stripping buffer (62.5 mM Tris–HCl, pH 6.7; 2% SDS; 100 mM 2-mecaptomethanol) at 50°C for 20 min. After being stripped, the membrane was washed three times in TBST.

Statistical analysis

Data are presented as means ± SEM. All experiments were undertaken in triplicate. Statistical significance was calculated with one-way ANOVA with Bonferroni's *post hoc* test. Significance was accepted at the level of $P < 0.05$. The data and statistical analysis comply with the recommendations on experimental design and analysis in pharmacology (Curtis *et al.,* 2015).

Materials

1-Methyl-4-pheynl-1,2,3,6-tetrahydropyridine (MPTP) hydrochloride, MPP^+ iodide, 3-(4,5-dimethylthiazol-2-yl)-2,5-diphenyltetrazolium bromide (MTT), EGTA, EDTA, NP-40, leupeptin, aprotinin, PMSF and okadaic acid were from Sigma-Aldrich (St. Louis, MO, USA). The antibodies anti-TH, anti-CD68 and anti-GFAP were from Abcam (Cambridge, MA, USA). The antibodies anti-**Bcl2**, anti-Bax, anti-phospho-**JNK** (p-JNK), anti-JNK, anti-cleaved **caspase 3**, anti-tubulin and anti-actin were purchased from Cell Signalling Technology (Beverley, MA, USA). cDNA Synthesis Kit, SYBR Green Supermix and Detergent-compatible protein assay kit were from Bio-Rad (Hercules, CA, USA). Neurobasal medium, DMEM, FBS and B27 were from Gibco (ThermoFisher Scientific). Chemiluminescence blotting

substrate was from Roche (Indianapolis, IN, USA). The other chemical reagents were of analytical grade.

Nomenclature of targets and ligands

Key protein targets and ligands in this article are hyperlinked to corresponding entries in http://www.guidetopharmacology.org, the common portal for data from the IUPHAR/BPS Guide to PHARMACOLOGY (Southan *et al.,* 2016), and are permanently archived in the Concise Guide to PHARMACOLOGY 2017/18 (Alexander *et al.,* 2017a,b).

Results

ABPPk improves cell viability and protects cells from apoptosis

To evaluate the potential protective roles of ABPPk in dopaminergic cells, we pretreated SH-SY5Y cells with ABPPk at different concentrations and then exposed the cells to MPP^+. The results showed that while the application of MPP^+ significantly reduced the cell viability, and the cells pretreated with ABPPk were resistant to the impairment (Figure 1A). To further ascertain these phenomena, we analysed released LDH activity. The results showed that LDH activity in the culture medium was markedly increased by MPP^+ (Figure 1B). As expected, this increase was largely counteracted by ABPPk (Figure 1B). We next wanted to examine whether similar protective effects of ABPPk could be observed in primary dopaminergic neurons. Indeed, pretreatment of ABPPk significantly improved neuron viability in the presence of MPP^+ (Figure 1C), and the application of ABPPk markedly attenuated the released LDH in the injured dopaminergic neurons (Figure 1D). Notably, these protective roles of ABPPk in SH-SY5Y cells and dopaminergic neurons were in a dose-dependent manner. These data clearly indicate that ABPPk possesses potent neuroprotective abilities against MPP^+ insult in dopaminergic neurons.

We next evaluated whether ABPPk protects cells from apoptosis by the TUNEL assay. Briefly, for this assay, Tunel staining recognizes the damaged DNA including double- and single-stranded DNA breaks. In SH-SY5Y cells, exposure to MPP^+ greatly induced cell apoptosis as evidenced by increases in the Tunel-positive cells (Figure 2A, B). However, the presence of ABPPk largely attenuated cell apoptosis induced by MPP^+ (Figure 2A, B). In primary dopaminergic neurons, the incubation of MPP^+ also induced cell apoptosis, but the application of ABPPk protected these cells from apoptosis (Figure 2C, D). These results further ascertained the anti-apoptotic abilities of ABPPk in dopaminergic neurons.

ABPPk increases Bcl2/Bax

Bcl2 is a major anti-apoptotic protein and Bax is a pro-apoptotic factor. It has been shown that the ratio of Bcl2 to Bax (Bcl2/Bax) determines cell fate (Mignard *et al.,* 2014). We thus measured the protein levels of Bcl2 and Bax by Western blot. In SH-SY5Y cells, ABPPk alone has no effect on the protein levels of Bcl2 and Bax (Figure 3A). When cells were exposed to MPP^+, the protein levels of Bcl2 and Bax were

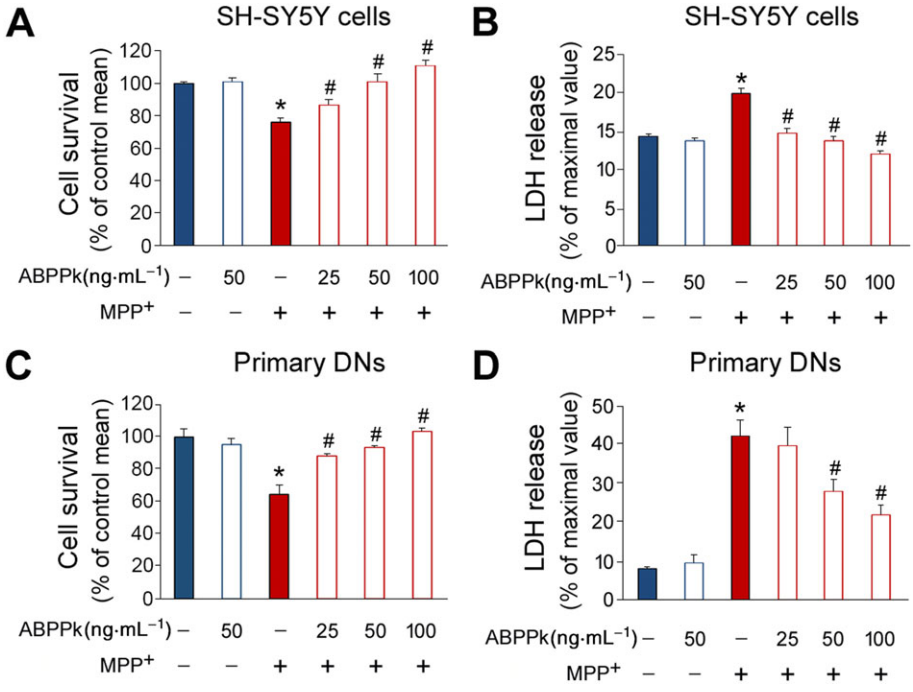

Figure 1

ABPPk increases cell viability in MPP^+-treated cells. (A, B) The SH-SY5Y cells were pretreated with ABPPk at different dosages and subjected to 500 μM MPP^+. The cell viability (A) and LDH activity in the culture medium (B) were analysed. (C, D) Results from rat primary dopaminergic neurons (DNs) pretreated with ABPPk at different dosages and subjected to 50 μM MPP^+. The cell viability (C) and LDH activity (D) were assayed. Error bars are ± SEM. $n = 5$. *$P < 0.05$ versus the vehicle treated cells. #$P < 0.05$ versus the cells treated with MPP^+ alone.

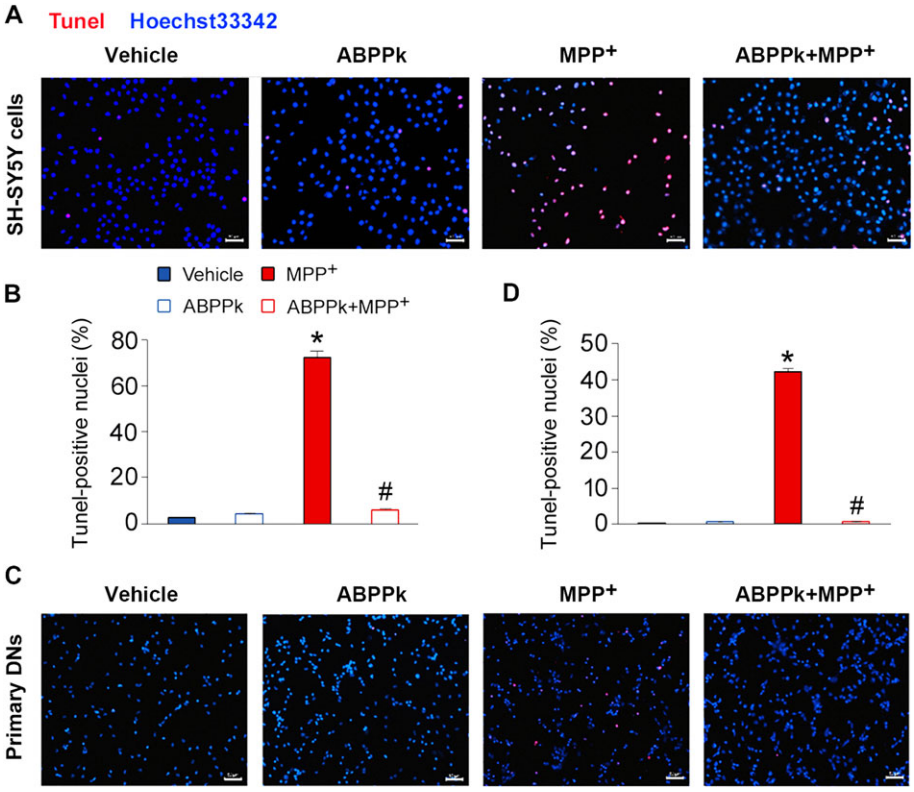

Figure 2

Tunel assays showing the protective effects of ABPPk. The SH-SY5Y cells (A, B) and primary dopaminergic neurons (DNs) (C, D) were pretreated with ABPPk at different dosages and exposed to 500 and 50 μM MPP^+ respectively. Cell apoptosis was measured by the Tunel assays. Tunel-positive cells (red) indicate apoptotic cells, and Hoechst33342 was used to stain the nuclei (blue). Scale bar = 50 μm. Error bars are ± SEM. $n = 5$. *$P < 0.05$ versus the vehicle treated cells. #$P < 0.05$ versus the cells treated with MPP^+ alone.

reduced and enhanced respectively (Figure 3A), leading to a dramatically down-regulated Bcl2/Bax. The pretreatment of ABPPk reversed this change, as the protein levels of Bcl2 and Bax were enhanced and reduced respectively, which resulted in an elevated Bcl2/Bax. Similarly, ABPPk pretreatment counteracted the effect of MPP^+, on Bcl2/Bax in the primary dopaminergic neurons (Figure 3B). Collectively, our results suggest that ABPPk protects cells from apoptosis by regulating the protein levels of Bcl2 and Bax.

ABPPk improves behavioural performances in MPTP-treated mice

The aforementioned results, which showed the potent neuroprotective roles of ABPPk in SH-SY5Y cells and dopaminergic neurons, prompted us to investigate whether ABPPk exhibits similar effects *in vivo*. We chose MPTP to induce mouse model of PD in this study. MPTP causes permanent symptoms of PD by destroying dopaminergic neurons in the SNpc and depleting dopamine level in the striatum (Onofrj and Ghilardi, 1990; Forno *et al.*, 1993). The experimental design was illustrated in Figure 4A. Rotarod test results showed that MPTP treatment significantly decreases the latency on rotarod. This impairment of latency was significantly improved by the application of ABPPk (Figure 4B). Furthermore, we performed pole test to measure the time taken by the mice to descend from the top of the pole to the floor. Elongated duration is considered to reflect bradykinesia. The injection of MPTP significantly increased the time to descend. However, ABPPk treatment almost completely abolished this elongation (Figure 4C). In the absence of MPTP, ABPPk application had no effect on these behavioural parameters both in rotarod and pole tests.

ABPPk prevents tyrosine hydroxylase (TH) loss in the SNpc

The beneficial roles of ABPPk in the MPTP-treated mice led us to hypothesize that ABPPk may protect dopaminergic neurons from MPTP-induced apoptosis. To test this hypothesis, we first analysed whether ABPPk treatment prevents general neuron loss induced by MPTP and Nissl staining was employed for this aim. The results showed that MPTP injection resulted in a great loss of neurons. The application of ABPPk almost completely reversed this decrease (Figure 5A, B). Next, we used immunohistochemistry method to evaluate whether ABPPk rescues dopaminergic neurons in MPTP-treated animals. To this aim, we analysed TH expression in the SNpc, as dopaminergic neurons are the main tissues for producing TH *in vivo*. As shown in Figure 5C, MPTP treatment induced a marked decrease in the TH-positive neurons. As expected, ABPPk treatment effectively prevented this decline

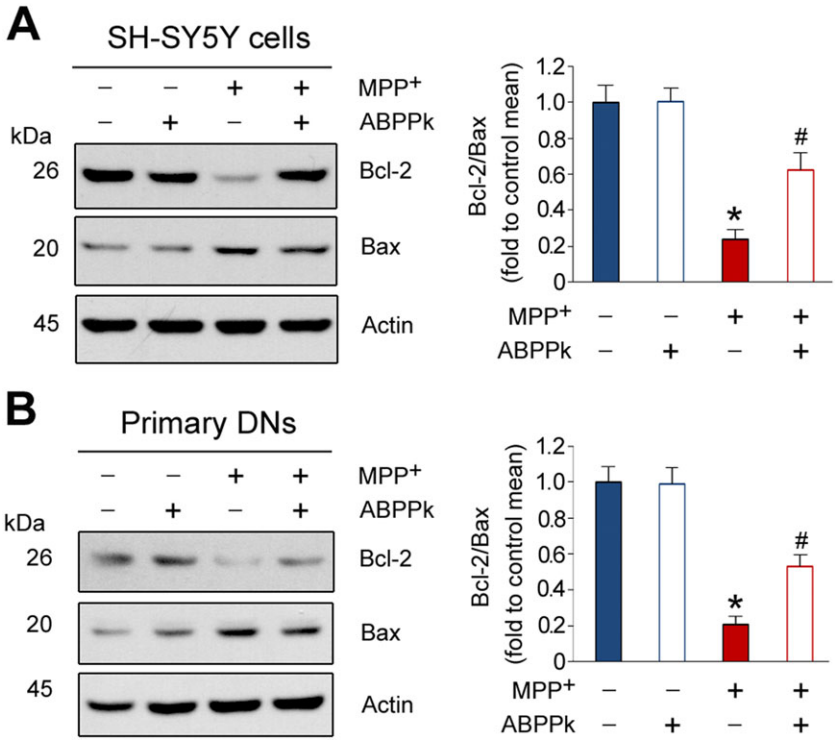

Figure 3

ABPPk increases the Bcl2/Bax ratio in the injured cells. The SH-SY5Y cells (A) and primary dopaminergic neurons (DNs) (B) were pretreated with 50 ng·mL^{-1} ABPPk and then exposed to 500 and 50 μM MPP$^+$, respectively, to induce cell apoptosis. The protein levels of Bcl2 and Bax were measured by Western blot with the antibodies as indicated. Actin was used as a loading control. Error bars are ± SEM. $n = 5$. *$P < 0.05$ versus the vehicle treated cells; #$P < 0.05$ versus the cells treated with MPP$^+$.

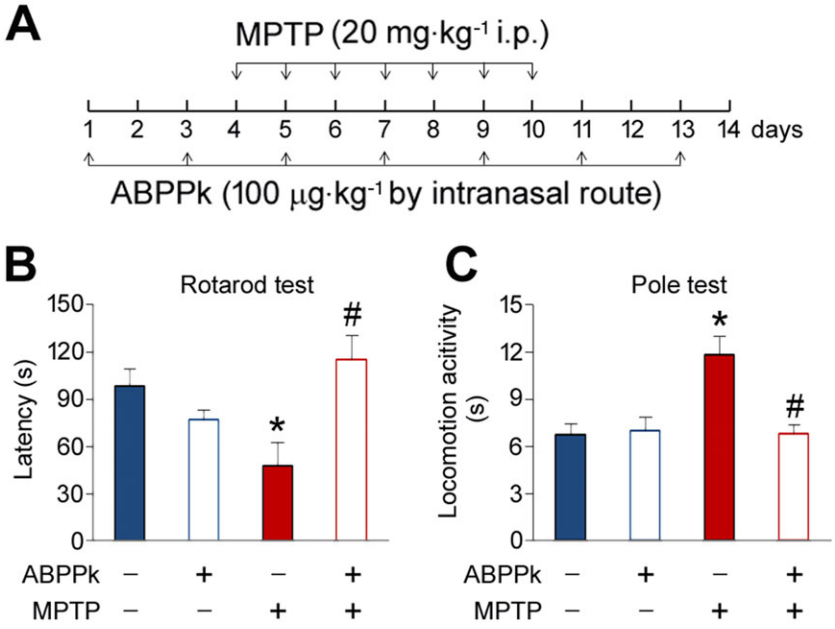

Figure 4

ABPPk attenuates MPTP-induced behavioural disorders. (A) Timeline of the experiments. (B) ABPPk improves rotarod performance in MPTP-treated mice. (C) ABPPk improves locomotor activity in MPTP-treated mice. Error bars are ± SEM. *$P < 0.05$ versus the vehicle treated mice. #$P < 0.05$ versus the mice treated with MPTP alone. $n = 5$ for each group.

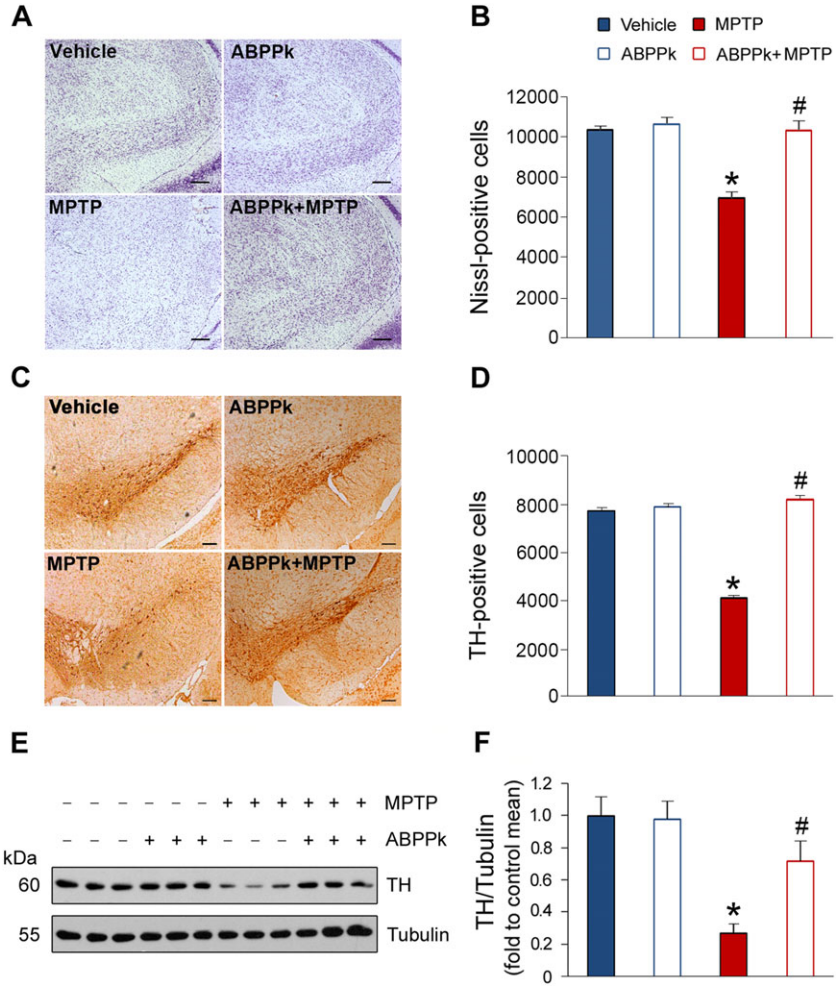

Figure 5

ABPPk prevents TH loss in the SNpc in MPTP-treated mice. (A) Nissl staining. Scale bar = 200 μm. (B) Number of Nissl positive cells, as shown in (A). (C) Immunohistochemical analysis of nigral dopaminergic neurons. Scale bar = 200 μm. (D) Stereological analysis of TH-positive neurons as shown in (C). (E) Western blot analysis of TH expression in the SNpc. Tubulin was used as a loading control. (F) Quantification of TH levels as illustrated in (E). Error bars are ± SEM. *$P < 0.05$ versus the vehicle treated mice; #$P < 0.05$ versus the mice treated with MPTP alone. $n = 5$ for each group.

(Figure 5C, D). To further confirm these findings, we measured TH protein levels by Western blot. Indeed, MPTP treatment causes a decrease in the TH protein levels, whereas ABPPk significantly counteracts this detrimental consequence (Figure 5E, F). Moreover, we also analysed TH expression in the striatum. The results showed that, as well as in the SNpc, ABPPk treatment greatly prevents MPTP-induced TH loss in the striatum (Figure 6A–D). These beneficial effects against MPTP-induced behavioural disorders and dopaminergic neuron loss were prolonged up to 10 days after the last ABPPk administration (Figure 7A–D).

ABPPk attenuates microglia and astrocyte activation

Chronic low-grade inflammation has been demonstrated as a principal causative factor for incidence of PD (Ransohoff, 2016). Microglia activation is responsible for the elevated neuroinflammation (Xiong *et al.*, 2016). To determine whether ABPPk modulates microglia activation and inflammation in the presence of MPTP, we evaluated microglia activation by immunostaining with the anti-CD68 antibody. As shown in Figure 8A, the CD68-positive cells were dramatically increased by MPTP exposure, which was largely blocked by the application of ABPPk (Figure 8A, B). In addition, astrocyte activation is also considered as an important factor for PD pathogenesis. GFAP is a commonly used marker of astrocyte activation. Our immunostaining showed that GFAP expression was robustly enhanced upon the MPTP treatment. However, such enhancement was greatly attenuated by ABPPk (Figure 8C, D). The changes in GFAP were further confirmed by Western blot (Figure 8E, F). These results suggest that ABPPk attenuates microglia and astrocyte activation induced by MPTP.

ABPPk down-regulates neuroinflammation and the apoptotic signalling pathways

Microglia and astrocyte activation is responsible for neuroinflammation (Xiong *et al.*, 2016). Thus, we examined

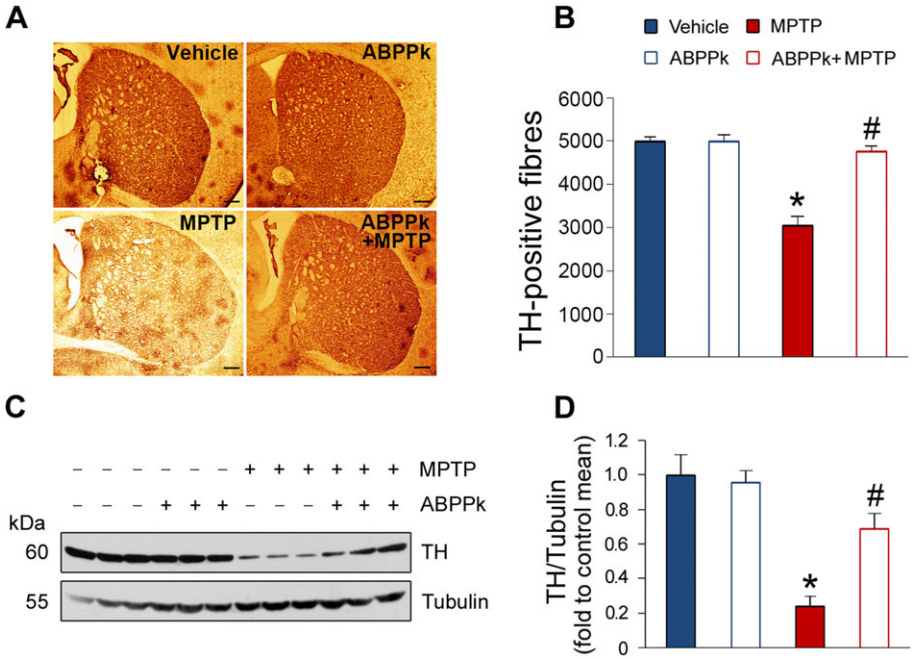

Figure 6

ABPPk prevents TH loss in the striatum in MPTP-treated mice. (A) Immunohistochemical analysis showing TH-positive fibres in the striatum. Scale bar = 250 μm. (B) Stereological analysis of TH-positive fibres as shown in (A). (C) Western blot analysis of TH expression in the striatum. Tubulin was used as a loading control. (D) Quantification of TH levels as shown in (C). *$P < 0.05$ versus the vehicle treated mice; #$P < 0.05$ versus the mice treated with MPTP alone. $n = 5$ for each group.

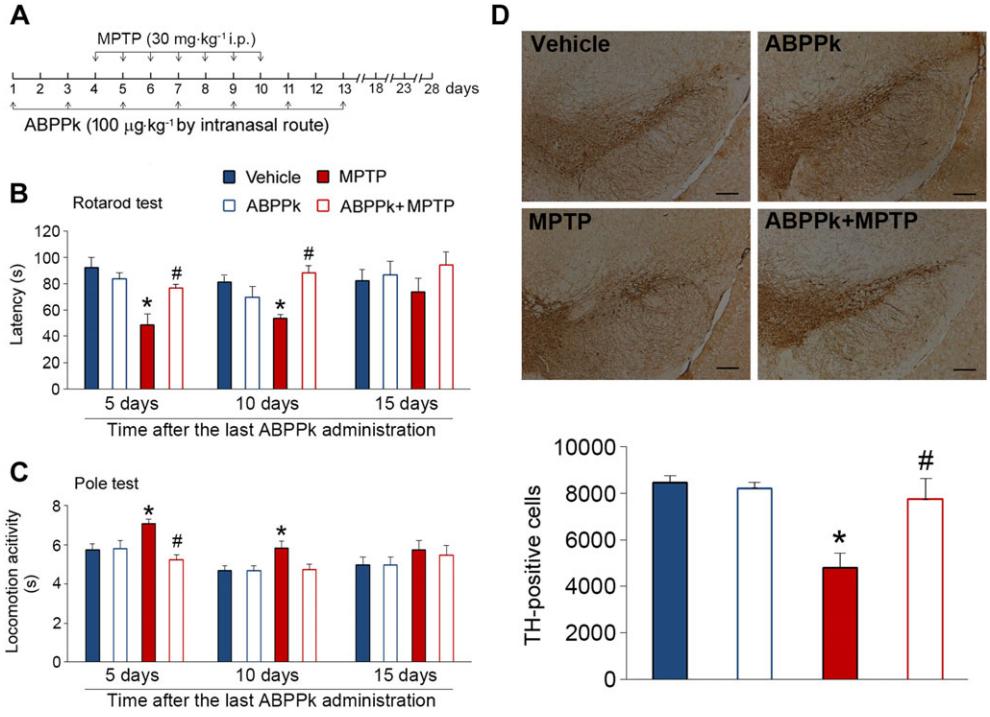

Figure 7

Long-term effects of ABPPk in MPTP-treated mice. (A) Timeline of the experiments. (B) ABPPk improves rotarod performance in MPTP-treated mice. (C) ABPPk improves locomotor activity in MPTP-treated mice. (D) Immunohistochemical analysis of nigral dopaminergic neurons. Samples were taken from mice at 10 days after the last ABPPk treatment. Scale bar = 100 μm. Error bars are ± SEM. *$P < 0.05$ versus the vehicle treated mice. #$P < 0.05$ versus the mice treated with MPTP alone. $n = 5$ for each group.

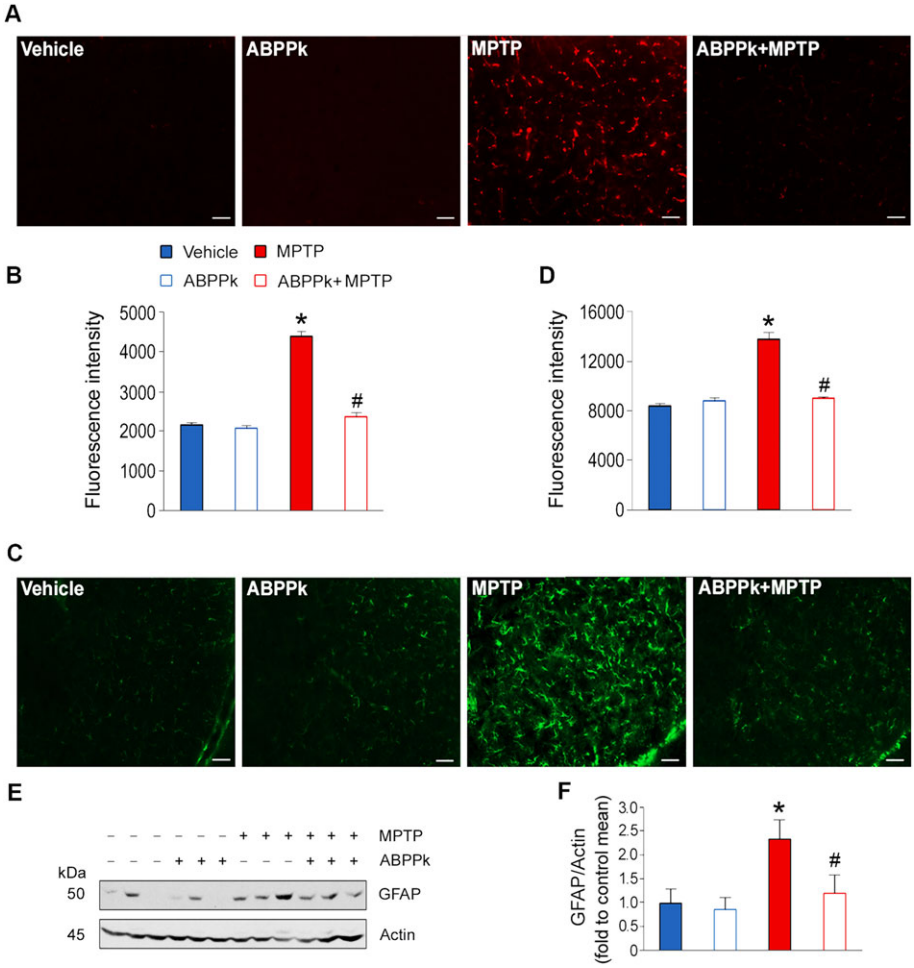

Figure 8

ABPPk attenuates microglia and astrocyte activation. (A) Immunostaining analysis of CD68 in the SNpc. (B) Quantification of the fluorescence intensity as shown in (A). (C) Immunostaining analysis of GFAP in the SNpc. (D) Quantification of the fluorescence intensity as shown in (C). (E) Western blot analysis of GFAP in the midbrain. Actin was used as a loading control. (F) Quantification of GFAP levels as illustrated in (E). Error bars are ± SEM. *$P < 0.05$ versus the vehicle treated mice; #$P < 0.05$ versus the mice treated with MPTP alone. Scale bar = 50 μm. $n = 5$ for each group.

inflammatory cytokine expression in the SNpc and striatum. The results showed that the mRNA levels of **IL-1α**, **IL-1β** and **IL-12A** were increased by MPTP treatment in the SNpc (Figure 9A). As compared to the MPTP-treated mice, ABPPk treatment significantly down-regulated the expression of these cytokines. Similar changes in IL-1α, IL-1β and IL-12A were observed in the striatum (Figure 9B). In addition, we also measured anti-inflammatory cytokine **IL-10** expression. The results showed that ABPPk increased the mRNA levels of IL-10 in the SNpc and striatum, especially in the presence of MPTP (Figure 9A, B). Since exposure to pro-inflammatory cytokines is known to induce cell apoptosis, we examined several protein levels involved in apoptotic signalling pathways. As shown in Figure 9C, the JNK activity was stimulated by MPTP, as evidenced by an increase in p-JNK. The application of ABPPk abolished this stimulation. As for Bcl-2/Bax, it was reduced by MPTP and the presence of ABPPk partially suppressed such reduction. MPTP-induced enhancement in cleaved caspase 3 was markedly counteracted by ABPPk (Figure 9C). These data indicate that ABPPk treatment attenuates neuroinflammation induced by MPTP and down-regulates the apoptotic signalling transduction.

Discussion

In this study, we pretreated SH-SH5Y cells and dopaminergic neurons with ABPPk, an active fraction isolated from traditional Chinese medicine *A. bidentata*, and observed that ABPPk markedly protected cells from apoptosis induced by MPP^+. Furthermore, in an *in vivo* PD mouse model, we found that ABPPk treatment significantly improves behavioural performances and prevents TH loss in the SNpc and striatum. Activation of microglia and astrocyte was greatly inhibited by ABPPk, which led to a decrease in pro-inflammatory cytokine expression. These data indicate that ABPPk has a potent neuroprotective role in dopaminergic neurons and might be used as a useful intervention against PD.

Extensive studies of *A. bidentata* suggest that it possesses multiple physiological functions, including adipogenesis

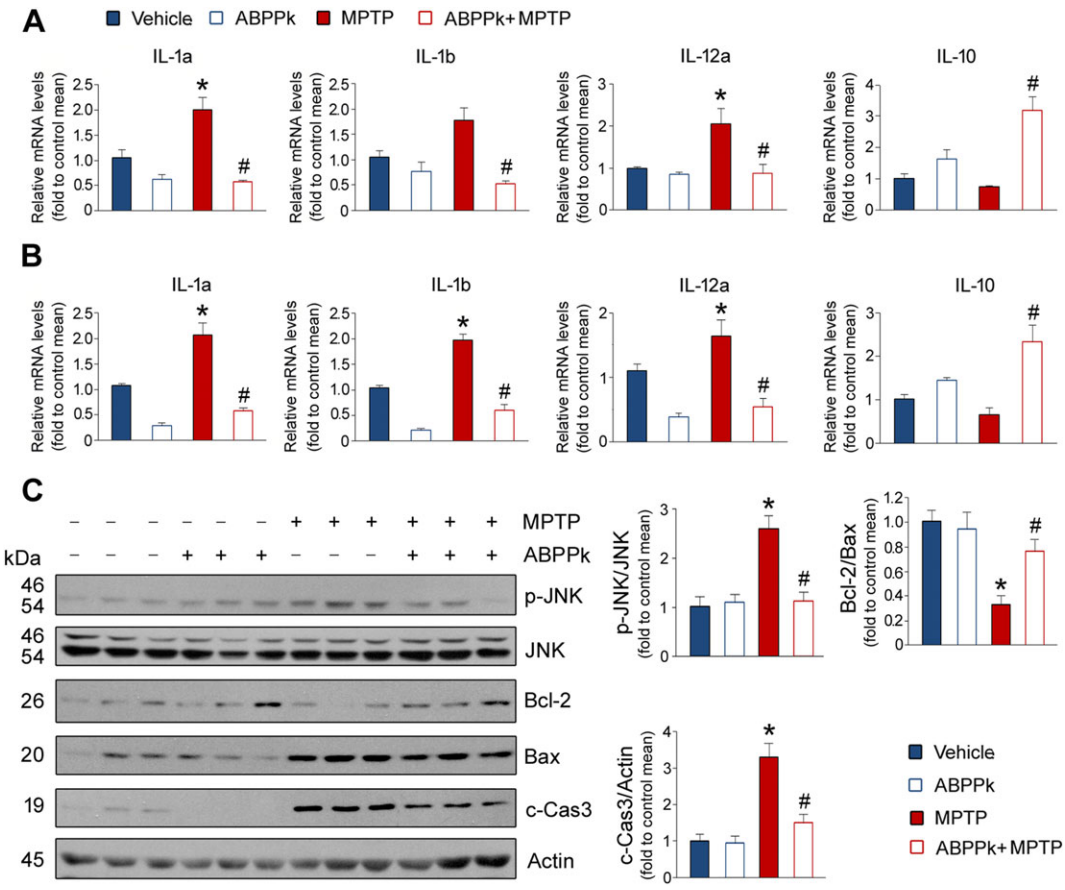

Figure 9

ABPPk down-regulates neuroinflammation and the apoptotic signalling transduction. (A) Inflammatory cytokine expression in the SNpc. (B) Inflammatory cytokine expression in the striatum. (C) Western blot analysis of the proteins involved in cell apoptotic signalling pathway. c-Cas3: cleaved capase3. Actin was used as a loading control. Error bars are ± SEM. *$P < 0.05$ versus the vehicle treated mice. #$P < 0.05$ versus the mice treated with MPTP alone. $n = 5$ for each group.

inhibition, anti-oxidative stress, promotion of osteogenic differentiation and chondrocyte proliferation (Tie *et al.,* 2013; Oh *et al.,* 2014; Suh *et al.,* 2014). Saponins and polysaccharides were considered as the two main constituents *A. bidentata* responsible for its pharmaceutical efficacies. Recently, we prepared polypeptide extraction from *A. bidentata* blume (ABPP) and found that ABPP exhibited neurotrophic and neuroprotective actions in several kinds of neurons (Shen *et al.,* 2008, 2013). To obtain the most potent fraction of ABPP, we separated the crude ABPP by HPLC and one fraction named ABPPk that showed the best neuroprotective actions both *in vitro* and *in vivo* (Cheng *et al.,* 2014; Yu *et al.,* 2014). In this study, we focused our interest on ABPPk and its potential applications for treating neuron loss associated diseases.

Since dopaminergic neuron loss is a main causative factor for developing PD, we hypothesized that ABPPk might play a beneficial role against PD by blocking neuron apoptosis. To test this hypothesis, we treated SH-SY5Y cells with ABPPk and then subjected the cells to MPP^+. As expected, ABPPk treatment significantly rescues the cells from apoptosis. Similarly, the MPP^+-induced cytotoxity was greatly attenuated by ABPPk in primary dopaminergic neurons. It should be noted that we used lower dosage of MPP^+ in primary neurons as compared to that in SH-SH5Y cells. This regimen was supported by previous report since the primary dopaminergic neurons were vulnerable to exogenous insults (Aime *et al.,* 2015). These findings were consistent with previous studies, which showed potent neuroprotective efficacies of ABPP in several different kinds of neurons that either were injured by various toxic agents or suffered from myocardial ischaemia (Shen *et al.,* 2008, 2010, 2011, 2013; Yu *et al.,* 2014). Recently, our group demonstrated that ABPPk could enhance neuronal growth *in vitro* and promote peripheral nerve regeneration after crush injury *in vivo* (Cheng *et al.,* 2014).

To further confirm the neuroprotective roles of ABPPk in cell models, we treated mice with MPTP *via* i.p. injection to induce PD model mice. MPTP is a lipophilic compound that can cross the blood–brain barrier and reach the brain where MPTP is metabolized into the toxic cation MPP^+ by the enzyme MAO-B. MPP^+ destroys primarily dopamine-producing neurons in the SNpc by interfering with complex I of the electron transports chain in mitochondria. Therefore, MPTP injection is an efficient strategy for inducing PD *in vivo* (Dauer and Przedborski, 2003; Filichia *et al.,* 2016). ABPPk is a polypeptide, which may not be able to cross the blood–brain barrier. To resolve this issue, we administrated

the mice with ABPPk *via* intranasal infusion. Previous studies have shown that intranasal infusion is an effective strategy for delivering drugs into the brain (Deng-Bryant *et al.,* 2016; Zhang *et al.,* 2016). Mice were pretreated with ABPPk and then subjected to MPTP injection for seven consecutive days. By this method, we successfully generated the PD mouse model, as evidenced by the impaired behavioural performance in the MPTP-treated mice. During MPTP injection, ABPPk was delivered every other day. As expected, the intranasal delivery of ABPPk improves those impaired behavioural performances. It is worthy to note that these behavioural and neuroprotective effects were up to 10 days after the last ABPPk treatment. TH is a key enzyme for producing dopamine, a precursor for the important neurotransmitters norepinephrine and epinephrine (Kaufman, 1995). TH loss is characteristic of PD, and we observed that ABPPk application largely prevents MPTP-mediated TH loss in the SNpc and striatum.

Increasing evidence shows that neuroinflammation plays a significant role in the pathogenesis of PD (Herrero *et al.,* 2015). Astrocyte and microglia are the two main cells for mediating neuroinflammation, and activation of either cell is known to be closely associated with neurotoxicity and neurodegeneration (Hirsch *et al.,* 2003). In agreement with these notions, we observed that MPTP treatment increases CD68- and GFAP-positive cells in the SNpc. ABPPk treatment greatly down-regulates astrocyte and microglia activation. Once astrocyte and microglia are activated, they will produce and secret a series of chemokines, which will in turn stimulate macrophage infiltration (Wrona, 2006). Together, activated microglia along with the recruitment of peripheral macrophages releases neurotoxic species such as pro-inflammatory cytokines and thus promotes neurodegeneration (Orr *et al.,* 2002). Indeed, the expression levels of IL-1α and IL-1β in the SNpc and striatum were elevated by MPTP, and these MPTP-induced events were abolished by ABPPk. Notably, the expression of the anti-inflammatory cytokine IL-10 is stimulated by ABPPk, especially in the SNpc. We speculate that M2 macrophages might be activated by ABPPk. Collectively, we conclude that ABPPk attenuates neuroinflammation in PD mice, which may be responsible for its neuroprotective roles *in vivo*. Currently, the structure of ABPPk is unknown. So future research needs to aim at solving the structure of ABPPk, and it will shed light on the molecular mechanisms underlying its neuroprotective roles. Moreover, the recombinant ABPPk will be developed by genetic engineering, which will pave the way for its clinical application in the future.

Acknowledgements

The authors would like to thank Dr. Xinhua Zhang for his technical guidance in tissue collection and immunohistochemistry. This work was supported by grants from the National Natural Science Foundation of China (nos 81471037 and 81770841), the Basic Research of Jiangsu Education Department (14KJA180006), the Six Talent Summit Project of Jiangsu Province (SWYY-051) and the Priority Academic Program Development (PAPD) of Jiangsu Higher Education Institutions.

Author contributions

X.G. conceived the research and provided ABPPk; C.S. designed and performed the experiments and analysed data; S.P., C.W., J.M., K.J. and Y.J. performed the experiments; C.S. wrote the manuscript with the input from all other authors.

Conflict of interest

The authors declare no conflicts of interest.

Declaration of transparency and scientific rigour

This Declaration acknowledges that this paper adheres to the principles for transparent reporting and scientific rigour of preclinical research recommended by funding agencies, publishers and other organisations engaged with supporting research.

References

Aime P, Sun X, Zareen N, Rao A, Berman Z, Volpicelli-Daley L *et al.* (2015). Trib3 is elevated in Parkinson's disease and mediates death in Parkinson's disease models. J Neurosci 35: 10731–10749.

Alam G, Edler M, Burchfield S, Richardson JR (2017). Single low doses of MPTP decrease tyrosine hydroxylase expression in the absence of overt neuron loss. Neurotoxicology 60: 99–106.

Alexander SPH, Kelly E, Marrion NV, Peters JA, Faccenda E, Harding SD *et al.* (2017a). The Concise Guide to PHARMACOLOGY 2017/18: Overview. Br J Pharmacol 174: S1–S16.

Alexander SPH, Fabbro D, Kelly E, Marrion NV, Peters JA, Faccenda E *et al.* (2017b). The Concise Guide to PHARMACOLOGY 2017/18: Enzymes. Br J Pharmacol 174: S272–S359.

Cheng Q, Jiang C, Wang C, Yu S, Zhang Q, Gu X *et al.* (2014). The *Achyranthes bidentata* polypeptide k fraction enhances neuronal growth *in vitro* and promotes peripheral nerve regeneration after crush injury *in vivo*. Neural Regen Res 9: 2142–2150.

Choi DY, Lee MK, Hong JT (2013). Lack of CCR5 modifies glial phenotypes and population of the nigral dopaminergic neurons, but not MPTP-induced dopaminergic neurodegeneration. Neurobiol Dis 49: 159–168.

Curtis MJ, Bond RA, Spina D, Ahluwalia A, Alexander SP, Giembycz MA *et al.* (2015). Experimental design and analysis and their reporting: new guidance for publication in BJP. Br J Pharmacol 172: 3461–3471.

Dauer W, Przedborski S (2003). Parkinson's disease: mechanisms and models. Neuron 39: 889–909.

Deng-Bryant Y, Readnower R, Leung LY, Tortella F, Shear D (2016). Methods of drug delivery in neurotrauma. Methods Mol Biol 1462: 89–100.

Filichia E, Hoffer B, Qi X, Luo Y (2016). Inhibition of Drp1 mitochondrial translocation provides neural protection in dopaminergic system in a Parkinson's disease model induced by MPTP. Sci Rep 6: 32656.

Forno LS, DeLanney LE, Irwin I, Langston JW (1993). Similarities and differences between MPTP-induced parkinsonsim and Parkinson's disease. Neuropathologic considerations. Adv Neurol 60: 600–608.

Franklin KBJ, Paxinos G (2008). The Mouse Brain. Academic Press: New York, NY.

Gandhi S, Wood-Kaczmar A, Yao Z, Plun-Favreau H, Deas E, Klupsch K *et al*. (2009). PINK1-associated Parkinson's disease is caused by neuronal vulnerability to calcium-induced cell death. Mol Cell 33: 627–638.

Goedert M (2015). NEURODEGENERATION. Alzheimer's and Parkinson's diseases: the prion concept in relation to assembled Abeta, tau, and alpha-synuclein. Science 349: 1255555.

He G, Guo W, Lou Z, Zhang H (2014). *Achyranthes bidentata* saponins promote osteogenic differentiation of bone marrow stromal cells through the ERK MAPK signaling pathway. Cell Biochem Biophys 70: 467–473.

Herrero MT, Estrada C, Maatouk L, Vyas S (2015). Inflammation in Parkinson's disease: role of glucocorticoids. Front Neuroanat 9: 32.

Hirsch EC, Breidert T, Rousselet E, Hunot S, Hartmann A, Michel PP (2003). The role of glial reaction and inflammation in Parkinson's disease. Ann N Y Acad Sci 991: 214–228.

Kaufman S (1995). Tyrosine hydroxylase. Adv Enzymol Relat Areas Mol Biol 70: 103–220.

Kilkenny C, Browne W, Cuthill IC, Emerson M, Altman DG (2010). Animal research: reporting *in vivo* experiments: the ARRIVE guidelines. Br J Pharmacol 160: 1577–1579.

Liu X, Zhao Y, Peng S, Zhang S, Wang M, Chen Y *et al*. (2016). BMP7 retards peripheral myelination by activating p38 MAPK in Schwann cells. Sci Rep 6: 31049.

Liu X, Peng S, Zhao Y, Zhao T, Wang M, Luo L *et al*. (2017). AMPK negatively regulates peripheral myelination via activation of c-Jun. Mol Neurobiol 54: 3554–3564.

Makin S (2016). Pathology: The prion principle. Nature 538: S13–S16.

McGrath JC, Lilley E (2015). Implementing guidelines on reporting research using animals (ARRIVE etc.): new requirements for publication in BJP. Br J Pharmacol 172: 3189–3193.

Mignard V, Lalier L, Paris F, Vallette FM (2014). Bioactive lipids and the control of Bax pro-apoptotic activity. Cell Death Dis 5: e1266.

Mortality GBD, Causes of Death C (2015). Global, regional, and national age-sex specific all-cause and cause-specific mortality for 240 causes of death, 1990-2013: a systematic analysis for the Global Burden of Disease Study 2013. Lancet 385: 117–171.

Nam JH, Park ES, Won SY, Lee YA, Kim KI, Jeong JY *et al*. (2015). TRPV1 on astrocytes rescues nigral dopamine neurons in Parkinson's disease via CNTF. Brain 138: 3610–3622. https://doi.org/10.1093/brain/awv297.

Oh SD, Kim M, Min BI, Choi GS, Kim SK, Bae H *et al*. (2014). Effect of *Achyranthes bidentata* blume on 3T3-L1 adipogenesis and rats fed with a high-fat diet. Evid Based Complement Alternat Med 2014: 158018–158017.

Onofrj M, Ghilardi MF (1990). MPTP induced parkinsonian syndrome: long term follow-up and neurophysiological study. Ital J Neurol Sci 11: 445–458.

Orr CF, Rowe DB, Halliday GM (2002). An inflammatory review of Parkinson's disease. Prog Neurobiol 68: 325–340.

Ransohoff RM (2016). How neuroinflammation contributes to neurodegeneration. Science 353: 777–783.

Shen H, Yuan Y, Ding F, Liu J, Gu X (2008). The protective effects of *Achyranthes bidentata* polypeptides against NMDA-induced cell apoptosis in cultured hippocampal neurons through differential modulation of NR2A- and NR2B-containing NMDA receptors. Brain Res Bull 77: 274–281.

Shen H, Yuan Y, Ding F, Hu N, Liu J, Gu X (2010). *Achyranthes bidentata* polypeptides confer neuroprotection through inhibition of reactive oxygen species production, Bax expression, and mitochondrial dysfunction induced by overstimulation of N-methyl-D-aspartate receptors. J Neurosci Res 88: 669–676.

Shen H, Wu X, Zhu Y, Sun H (2013). Intravenous administration of *Achyranthes bidentata* polypeptides supports recovery from experimental ischemic stroke *in vivo*. PLoS One 8: e57055.

Shen Y, Zhang Q, Gao X, Ding F (2011). An active fraction of *Achyranthes bidentata* polypeptides prevents apoptosis induced by serum deprivation in SH-SY5Y cells through activation of PI3K/Akt/Gsk3beta pathways. Neurochem Res 36: 2186–2194.

Southan C, Sharman JL, Benson HE, Faccenda E, Pawson AJ, Alexander SPH *et al*. (2016). The IUPHAR/BPS guide to PHARMACOLOGY in 2016: towards curated quantitative interactions between 1300 protein targets and 6000 ligands. Nucl Acids Res 44: D1054–D1068.

Suh KS, Lee YS, Choi EM (2014). The protective effects of *Achyranthes bidentata* root extract on the antimycin A induced damage of osteoblastic MC3T3-E1 cells. Cytotechnology 66: 925–935.

Sun C, Wang M, Liu X, Luo L, Li K, Zhang S *et al*. (2014). PCAF improves glucose homeostasis by suppressing the gluconeogenic activity of PGC-1alpha. Cell Rep 9: 2250–2262.

Tie R, Ji L, Nan Y, Wang W, Liang X, Tian F *et al*. (2013). *Achyranthes bidentata* polypeptides reduces oxidative stress and exerts protective effects against myocardial ischemic/reperfusion injury in rats. Int J Mol Sci 14: 19792–19804.

Wang Y, Shen W, Yang L, Zhao H, Gu W, Yuan Y (2013). The protective effects of *Achyranthes bidentata* polypeptides on rat sciatic nerve crush injury causes modulation of neurotrophic factors. Neurochem Res 38: 538–546.

Wrona D (2006). Neural-immune interactions: an integrative view of the bidirectional relationship between the brain and immune systems. J Neuroimmunol 172: 38–58.

Xie X, Zhao Y, Ma CY, Xu XM, Zhang YQ, Wang CG *et al*. (2015). Dimethyl fumarate induces necroptosis in colon cancer cells through GSH depletion/ROS increase/MAPKs activation pathway. Br J Pharmacol 172: 3929–3943.

Xiong XY, Liu L, Yang QW (2016). Functions and mechanisms of microglia/macrophages in neuroinflammation and neurogenesis after stroke. Prog Neurobiol 142: 23–44.

Ye Q, Huang W, Li D, Si E, Wang J, Wang Y*et al*. (2016). Overexpression of PGC-1alpha influences mitochondrial signal transduction of dopaminergic neurons. Mol Neurobiol 53: 3756–3770.

Yu S, Wang C, Cheng Q, Xu H, Zhang S, Li L *et al*. (2014). An active component of *Achyranthes bidentata* polypeptides provides neuroprotection through inhibition of mitochondrial-dependent apoptotic pathway in cultured neurons and in animal models of cerebral ischemia. PLoS One 9: e109923.

Yuan Y, Shen H, Yao J, Hu N, Ding F, Gu X (2010). The protective effects of *Achyranthes bidentata* polypeptides in an experimental model of mouse sciatic nerve crush injury. Brain Res Bull 81: 25–32.

Zhang Y, Dai CL, Chen Y, Iqbal K, Liu F, Gong CX (2016). Intranasal insulin prevents anesthesia-induced spatial learning and memory deficit in mice. Sci Rep 6: 21186.

Zou Y, Meng J, Chen W, Liu J, Li X, Li W*et al*. (2011). Modulation of phenotypic and functional maturation of murine dendritic cells (DCs) by purified *Achyranthes bidentata* polysaccharide (ABP). Int Immunopharmacol 11: 1103–1108.